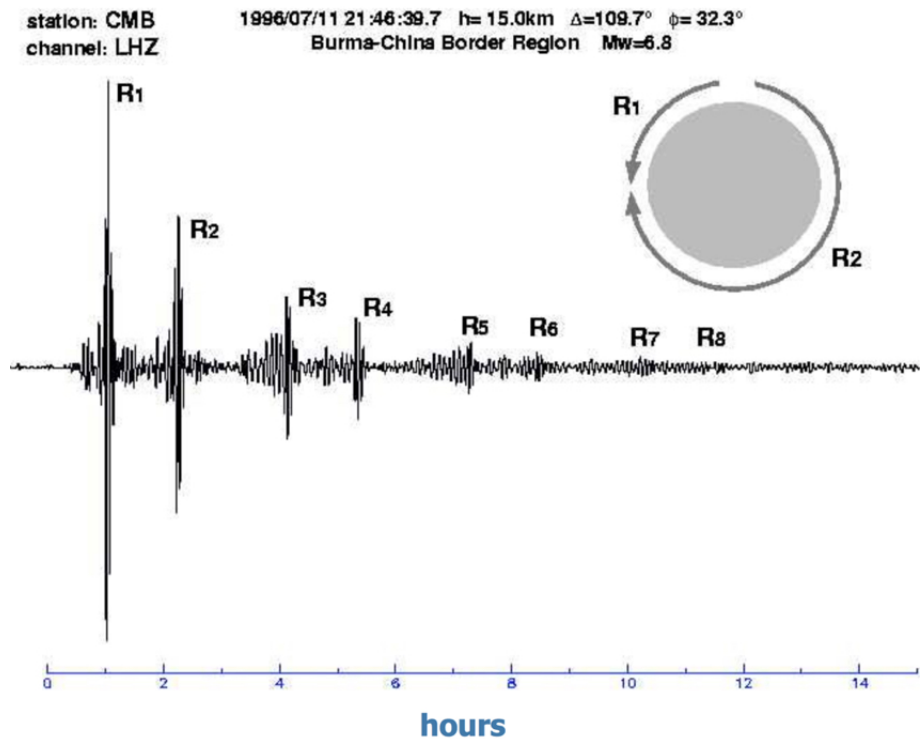


4 The Basic Properties of Surface Waves



Rayleigh wave arrivals recorded on the vertical component
at a station with 109° epicentral distance.

Introduction

Whenever an elastic medium is bounded by a free surface, coherent waves arise that travel along that surface; the amplitude of those surface waves decays with increasing distance from the surface (that is to say, in the Earth, with increasing depth). Two distinct types of surface waves are observed: *Love waves*, whose associated displacement is parallel to the free surface and perpendicular to the direction of propagation, and *Rayleigh waves*, with displacement on a plane perpendicular to Love-wave displacement. The speed with which surface waves propagate is related to, but does not coincide with, compressional and/or shear velocities in the region of the medium close to the free surface (in the Earth, the crust and upper mantle).

In the following chapter, we will investigate surface waves as solutions to the equations of motions. For illustration purposes, we will focus on Love waves since they are slightly easier to treat and understand in a mathematical sense.

Learn objectives

- You know the characteristics of Love and Rayleigh waves.
- You are able to explain how Love waves are generated in an elastic medium.
- You are familiar with the dispersion of surface waves.

4.1 Observations of Love and Rayleigh Waves

Observations of surface waves (figure 4.1) show in particular two different types of particle motions. Surface waves are thus separated into *Love waves*, with displacement parallel to the free surface and perpendicular to the direction of propagation, and *Rayleigh waves*, with displacement on a plane perpendicular to Love-wave displacement (figure 4.2).

Figure 2.7-1: Seismograms recorded at a distance of 110°, showing surface waves.

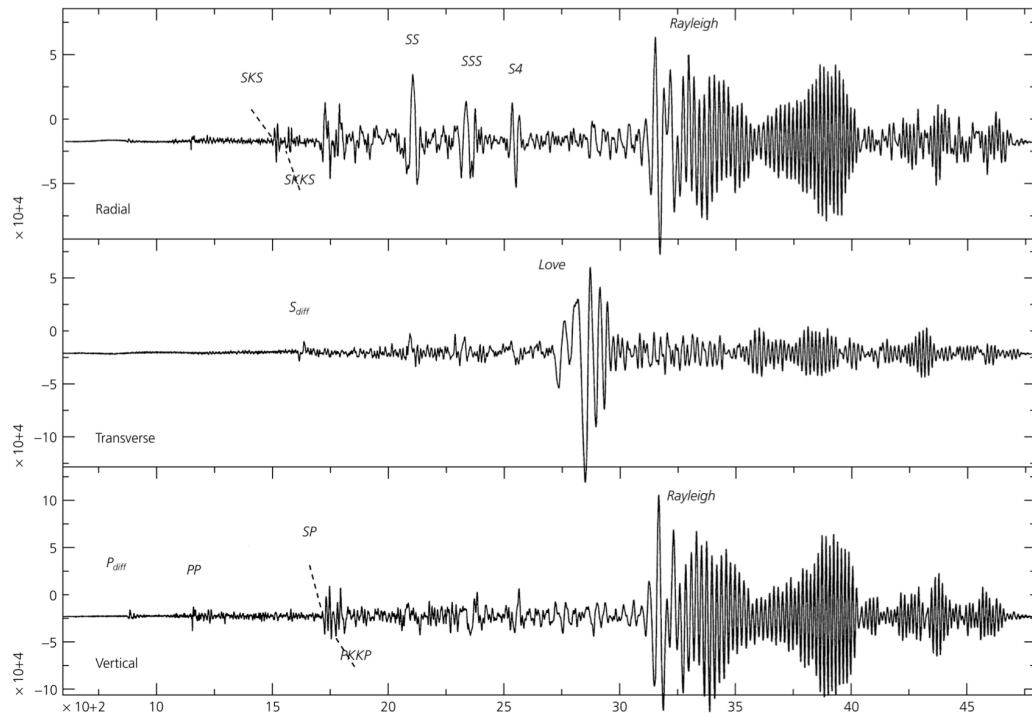


Figure 4.1: (From Stein & Wysession) Distinct surface waves are observed on the vertical, radial and transverse components of a seismogram. The vertical and radial components (P and SV motion) are clearly correlated: they are horizontal and vertical displacements associated with the same propagating wave, that seismologists have called *Rayleigh wave*. The surface wave observed on the transverse (SH motion) component of the seismogram has a different character, and propagates at different speed. It is called *Love wave*.

4.2 Love Waves

Example of Love-Wave Solution to the Equation of Motion: From a Vectorial to a Scalar Equation

In a Cartesian reference frame $\mathbf{r} = (x_1, x_2, x_3)$, with x_1 the direction of propagation and x_3 the direction of increasing depth, a Love-wave displacement like that sketched in figure 4.2 (top) can be written

$$\mathbf{u}(\mathbf{r}, t) = \left(0, h(x_3) e^{i(kx_1 - \omega t)}, 0 \right), \quad (4.1)$$

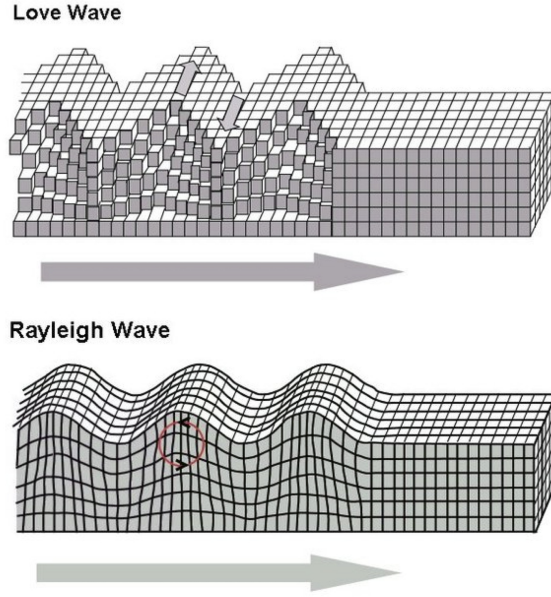


Figure 4.2: (From *Fowler*) The displacement associated with Love waves is perpendicular to the direction of propagation, and parallel to the Earth's surface; the displacement associated with Rayleigh waves lies in the plane parallel to the direction of propagation, and perpendicular to the Earth's surface.

with i the imaginary unit, ω (frequency) and k (“wavenumber”, i.e. ratio of frequency to phase velocity) arbitrary constants, and the unknown function $h(x_3)$ meant to describe the decay of displacement (by definition of surface wave) with increasing depth below the surface.

Let the medium be elastic, with constitutive relation

$$\tau_{ij} = \lambda \frac{\partial u_k}{\partial x_k} + \mu \left(\frac{\partial u_i}{\partial x_j} + \frac{\partial u_j}{\partial x_i} \right). \quad (4.2)$$

Since, according to eq. (4.1), we are only interested in displacements in the x_2 direction, and not depending on x_2 itself, we can substitute $u_1 = u_3 = \frac{\partial u_2}{\partial x_2} = 0$ in (4.2), which then collapses to

$$\tau_{ij} = \mu \left(\frac{\partial u_i}{\partial x_j} + \frac{\partial u_j}{\partial x_i} \right). \quad (4.3)$$

Accordingly, the equation of motion (see previous lectures)

$$\rho \frac{\partial^2 u_i}{\partial t^2} = \frac{\partial \tau_{ji}}{\partial x_j} \quad (4.4)$$

can be written

$$\rho \frac{\partial^2 u_i}{\partial t^2} = \mu \frac{\partial}{\partial x_j} \left(\frac{\partial u_i}{\partial x_j} + \frac{\partial u_j}{\partial x_i} \right), \quad (4.5)$$

or, after substituting, again, $u_1 = u_3 = \frac{\partial u_2}{\partial x_2} = 0$,

$$\rho \frac{\partial^2 u_2}{\partial t^2} = \mu \left(\frac{\partial^2 u_2}{\partial x_1^2} + \frac{\partial^2 u_2}{\partial x_3^2} \right). \quad (4.6)$$

General Love-Wave Solution: Layer Over Half-Space Model

Consider an extremely simplified model of the Earth as a homogeneous layer (the crust) of thickness H overlying a homogeneous half-space (the upper mantle). Let us call ρ_1 and μ_1 the density and rigidity of the layer, and ρ_2 and μ_2 those of the half-space. Shear velocity $\beta = \mu/\rho$ is higher in the mantle than in the crust, so we assume $\beta_1 = \sqrt{\mu_1/\rho_1} \leq \beta_2 = \sqrt{\mu_2/\rho_2}$.

For both the layer and half-space, let us substitute the Love-wave *Ansatz* (4.1) into the equation of motion (4.6). The term $e^{i(kx_1 - \omega t)}$ cancels out, and we find

$$\frac{\partial^2 h(x_3)}{\partial x_3^2} = \left(k^2 - \frac{\omega^2}{\beta_i^2} \right) h(x_3), \quad (4.7)$$

for $i = 1, 2$ (both layer and half-space). It can be verified that a complete solution to (4.7) is

$$h_i(x_3) = A_i e^{-\sqrt{k^2 - \omega^2/\beta_i^2} x_3} + B_i e^{+\sqrt{k^2 - \omega^2/\beta_i^2} x_3} \quad (i = 1, 2), \quad (4.8)$$

where the arbitrary constants A_i and B_i are to be determined via the boundary conditions, and will have different values in the layer vs. the half-space (hence the subscript i).

Substituting (4.8) into (4.1), we find the general solution for displacement

$$u_2(\mathbf{r}, t) = \left[A_i e^{-\sqrt{k^2 - \omega^2/\beta_i^2} x_3} + B_i e^{+\sqrt{k^2 - \omega^2/\beta_i^2} x_3} \right] e^{i(kx_1 - \omega t)} \quad (i = 1, 2) \quad (4.9)$$

Boundary Conditions

The quantities A_1 , B_1 , A_2 , B_2 , k and ω can be constrained applying realistic boundary conditions, namely: (i) that displacements tend to zero when $x_3 \rightarrow \infty$ (no seismic sources below a certain depth); (ii) that the outer surface be free of stresses; (iii) that displacements and tractions be continuous at the interface $x_3 = H$ between layer and half-space.

The boundary condition (i) is satisfied if we require either $\text{Re}(-\sqrt{k^2 - \omega^2/\beta_2^2}) < 0$, and $B_2=0$, or $\text{Re}(+\sqrt{k^2 - \omega^2/\beta_2^2}) < 0$, and $A_2=0$. Let us pick the first option. Notice that this condition only affects the half-space solution ($i = 2$).

The condition (ii) can be written $\tau_{31} = \tau_{32} = \tau_{33} = 0$. We already know that $\tau_{31} = \tau_{33} = 0$ since $u_1 = u_3 = 0$ by construction, while $\tau_{32} = \mu \left(\frac{\partial u_2}{\partial x_3} \right)$. We are then left with the condition $\frac{\partial u_2}{\partial x_3} = 0$, or

$$\left[-\sqrt{k^2 - \omega^2/\beta_1^2} A_1 e^{-\sqrt{k^2 - \omega^2/\beta_1^2} x_3} + \sqrt{k^2 - \omega^2/\beta_1^2} B_1 e^{+\sqrt{k^2 - \omega^2/\beta_1^2} x_3} \right] e^{i(kx_1 - \omega t)} = 0 \quad (4.10)$$

at all times t , hence $A_1 = B_1$. This condition only affects the top-layer solution ($i = 1$).

Before imposing the condition (iii), notice that the solution in the top layer can now be written in the simpler form

$$\begin{aligned} u_2(\mathbf{r}, t) &= A_1 \left[e^{-\sqrt{k^2 - \omega^2/\beta_1^2} x_3} + e^{+\sqrt{k^2 - \omega^2/\beta_1^2} x_3} \right] e^{i(kx_1 - \omega t)} \\ &= 2A_1 \cos \left(i\sqrt{k^2 - \omega^2/\beta_1^2} x_3 \right) e^{i(kx_1 - \omega t)} \end{aligned} \quad (4.11)$$

and in the half-space

$$u_2(\mathbf{r}, t) = A_2 e^{-\sqrt{k^2 - \omega^2/\beta_2^2} x_3} e^{i(kx_1 - \omega t)}. \quad (4.12)$$

Condition (iii) includes continuity of displacements at $x_3 = H$, i.e.

$$2A_1 \cos \left(i\sqrt{k^2 - \omega^2/\beta_1^2} H \right) = A_2 e^{-\sqrt{k^2 - \omega^2/\beta_2^2} H} \quad (4.13)$$

(after dividing both sides by the time-dependent exponential), and continuity of tractions, i.e. (see discussion of condition (ii) above) of $\mu \left(\frac{\partial u_2}{\partial x_3} \right)$, which means

$$2\mu_1 A_1 i\sqrt{k^2 - \omega^2/\beta_1^2} \sin \left(i\sqrt{k^2 - \omega^2/\beta_1^2} H \right) = \mu_2 \sqrt{k^2 - \omega^2/\beta_2^2} A_2 e^{-\sqrt{k^2 - \omega^2/\beta_2^2} H}. \quad (4.14)$$

We have no more boundary conditions left, and the two equations (4.13) and (4.14) are not sufficient to determine the four, still arbitrary parameters A_1 , A_2 , ω and k uniquely. This means that the physical problem we are facing does not have a single solution, but rather a spectrum of solutions (*eigenvalue problem*).

Love-Wave “Modes”

From (4.13) and (4.14), let us find two expressions for the ratio A_2/A_1 ; requiring that their values coincide, we find

$$\frac{2 \cos \left(i\sqrt{k^2 - \omega^2/\beta_1^2} H \right)}{e^{-\sqrt{k^2 - \omega^2/\beta_2^2} H}} = \frac{2\mu_1 i\sqrt{k^2 - \omega^2/\beta_1^2} \sin \left(i\sqrt{k^2 - \omega^2/\beta_1^2} H \right)}{\mu_2 \sqrt{k^2 - \omega^2/\beta_2^2} e^{-\sqrt{k^2 - \omega^2/\beta_2^2} H}}. \quad (4.15)$$

After some algebra,

$$\tan \left(i\sqrt{k^2 - \omega^2/\beta_1^2} H \right) = \frac{\mu_2 \sqrt{k^2 - \omega^2/\beta_2^2}}{\mu_1 i\sqrt{k^2 - \omega^2/\beta_1^2}}. \quad (4.16)$$

The following treatment is more intuitive if one substitutes $k = \omega/c$, where it is apparent from equation (4.1) that c has the meaning of phase velocity. We then rewrite (4.16)

$$\tan \left(i\omega H \sqrt{\frac{1}{c^2} - \frac{1}{\beta_1^2}} \right) = \frac{\mu_2 \sqrt{\frac{1}{c^2} - \frac{1}{\beta_2^2}}}{\mu_1 i\sqrt{\frac{1}{c^2} - \frac{1}{\beta_1^2}}}, \quad (4.17)$$

or equivalently

$$\tan \left(\omega H \sqrt{\frac{1}{\beta_1^2} - \frac{1}{c^2}} \right) = \frac{\mu_2 \sqrt{\frac{1}{c^2} - \frac{1}{\beta_2^2}}}{\mu_1 \sqrt{\frac{1}{\beta_1^2} - \frac{1}{c^2}}}. \quad (4.18)$$

In principle, given ω , we can use (4.18) to find a set of values of c for which a solution (4.11), (4.12) exists (other quantities in (4.18), i.e. μ_1 , μ_2 , β_1 , β_2 , H , are fixed). It is apparent from (4.18) that real solutions for c only exist between β_1 and β_2 , i.e. $\beta_1 < c < \beta_2$.

Let us study *graphically* (i.e., numerically) the properties of (4.18) and of its solutions ω ,

c. After defining $X = H\sqrt{1/\beta_1^2 - 1/c^2}$ (4.18) becomes

$$\tan(\omega X) = \frac{\mu_2 \sqrt{\frac{H}{\beta_1^2} - \frac{H}{\beta_2^2} - X^2}}{\mu_1 X}. \quad (4.19)$$

The left-hand and right-hand sides of (4.19) are sketched in figure 4.3 for a fixed, unspecified value of ω . The right-hand side is always positive within the interval of interest, $\beta_1 < c < \beta_2$. It tends to ∞ for $X \rightarrow 0$, that is to say $c \rightarrow \beta_1$ (importantly, this implies that we shall find no solution $c < \beta_1$). It equals 0 when $c = \beta_2$, i.e. at the opposite end of the interval $\beta_1 < c < \beta_2$. Each intersection between the left-hand side and right-hand side, within the interval $\beta_1 < c < \beta_2$, corresponds to a real value of c for which a solution to (4.6) exists, satisfying the boundary conditions for the given value of ω .

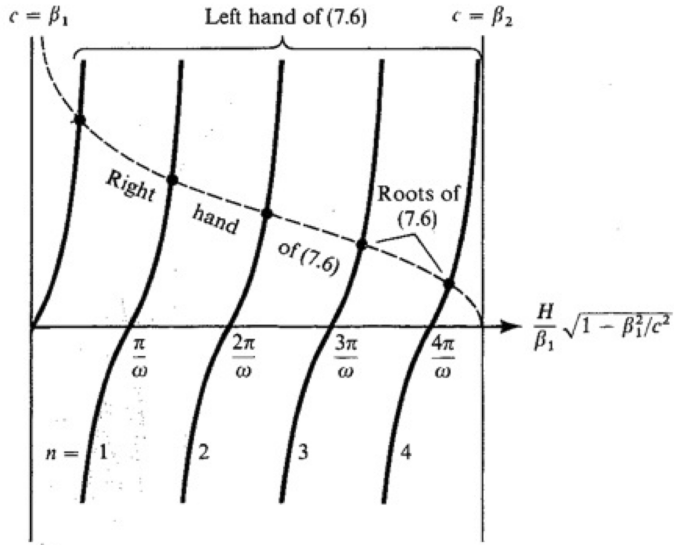


Figure 4.3: Left-hand and right-hand sides of eq. (4.19). Intersections identify possible values of phase velocity c at frequency ω , i.e. surface wave "modes". (From Aki & Richards. Eq. (7.6) of Aki & Richards is equivalent to eq. (4.18) and (4.19) here)

We can infer from figure 4.3 that, for a given ω , the number of possible solutions (eigenvalues) (ω, c) grows with the maximum interesting value of X , that is to say with $H\sqrt{1/\beta_1^2 - 1/\beta_2^2}$; hence with the difference between β_1 and β_2 . The lowest- c solution is called "fundamental mode" surface wave; additional solutions are dubbed "overtones", and ordered (first overtone, second overtone, etc.) by increasing velocity. The total number of possible overtones depends on the number of cycles of $\tan(\omega X)$ within the interval of X -values corresponding to $\beta_1 < c < \beta_2$. This in turn depends on the value of ω . We can find the value of ω corresponding to one full cycle, if we replace $c = \beta_2$ in the argument of \tan at the left-hand side of (4.19), and equate it to π ,

$$\frac{\pi}{\omega_{c1}} = H \sqrt{\frac{1}{\beta_1^2} - \frac{1}{\beta_2^2}}, \quad (4.20)$$

and

$$\omega_{c1} = \frac{\pi}{H \sqrt{\frac{1}{\beta_1^2} - \frac{1}{\beta_2^2}}}, \quad (4.21)$$

where the subscript $c1$ reminds us that ω_{c1} is the cut-off frequency for the first mode.

Likewise, n modes can only exist for values of ω bigger than

$$\omega_{cn} = \frac{n\pi}{H \sqrt{\frac{1}{\beta_1^2} - \frac{1}{\beta_2^2}}} \quad (4.22)$$

(simply replace π with $n\pi$ in (4.20)); ω_{cn} is accordingly dubbed “*cut-off frequency*” for the n -th mode.

Possible values of phase velocity c at a given frequency can be identified numerically as sketched in figure 4.3. Solutions (ω, c) of (4.19) can be substituted into (4.11) and (4.12), using $k = \omega/c$, to find the general Love wave solution satisfying all boundary conditions. For any given values of x_1 and t we can sketch the vertical behavior of $u_2(x_1, x_3, t)$ (the radial eigenfunction $h(x_3)$ corresponding to the values (ω, c) in question): examples at cut-off and higher frequencies are sketched in figure 4.4. The number of zero-crossings in the vertical direction coincides with the integer number n defined above.

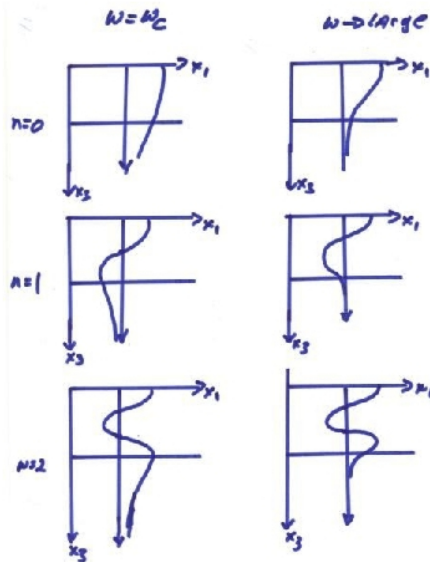


Figure 4.4: Love-wave displacement changes in the vertical direction, at any time t and location x_1 , in a layer-over-half-space model. Zero-crossings are limited to the top layer, where the radial-depending factor in u_2 is oscillatory. (From the lecture notes of R. Nowack at Purdue University)

4.3 Rayleigh waves

A similar treatment (algebraically more complicated) can be applied to a Rayleigh-wave trial solution (displacement along the x_1 and x_3 , with propagation along the x_1 axis). See, for example, *Aki & Richards* (2002). Not surprisingly, Rayleigh-wave velocity turns out to depend on both compressional and shear body-wave speeds.

4.4 Dispersion, phase velocity, group velocity

In the previous section we have seen mathematically that Love (and Rayleigh) waves in a layer-over-half-space model can exist at all frequencies. At each frequency, only a discrete set of phase velocities is possible. For a given value of n , we can plot acceptable values of c versus ω (figure 4.5).

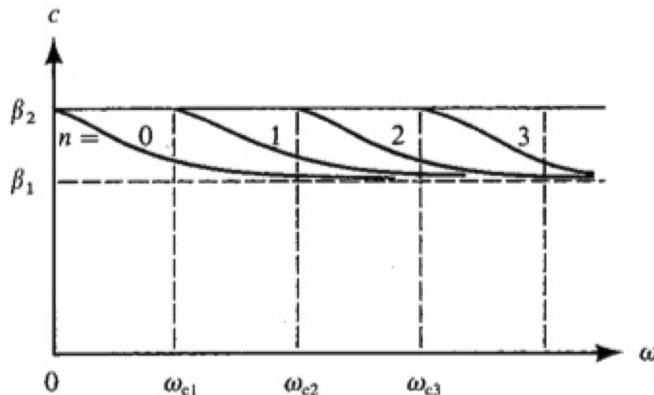


Figure 4.5: Phase velocity c vs. frequency ω , for different values of n . Plots like this are called *dispersion curves*. (From *Aki & Richards*)

The dependence of phase velocity on the frequency of a propagating wave is a phenomenon known as *dispersion*, and "easily" observed on seismograms (figure 4.6).

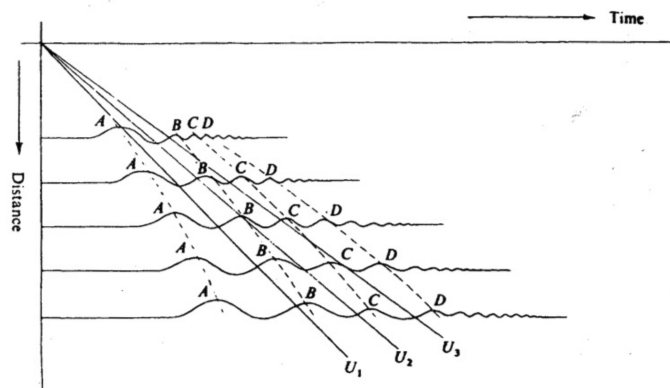


Figure 4.6: Dispersion of a surface-wavepacket. (From *Lay & Wallace*)

A consequence of dispersion is the existence of wavepackets such as that illustrated in figure 4.6: the surface-wave envelope has itself a sinusoidal shape, and propagates with its own speed called "*group velocity*". In the absence of dispersion, group and phase velocity coincide. We illustrate these concepts first with a heuristic example, then with a more complex derivation.

The concept of group velocity: a simple example

Let us consider the simple case of two surface wave modes that propagate with the same amplitude at slightly different frequencies $\omega + \delta\omega$ and $\omega - \delta\omega$. Corresponding wavenumbers are $k - \delta k$ and $k + \delta k$, respectively (remember $k = \omega/c$). For simplicity, we only consider the cosine terms of each mode, and write the total displacement as their sum,

$$u_2 = \cos[(\omega - \delta\omega)t - (k - \delta k)x_1] + \cos[(\omega + \delta\omega)t - (k + \delta k)x_1], \quad (4.23)$$

which can then be rewritten

$$\begin{aligned} u_2 &= \cos[(\omega t - kx_1) - (\delta\omega t - \delta kx_1)] + \cos[(\omega t - kx_1) + (\delta\omega t - \delta kx_1)] \\ &= 2 \cos(\omega t - kx_1) \cos(\delta\omega t - \delta kx_1), \end{aligned} \quad (4.24)$$

thanks to the property of the cosine, $\cos(\alpha + \beta) + \cos(\alpha - \beta) = 2 \cos \alpha \cos \beta$. Equation (4.24), illustrated graphically in figure 4.7, shows that, when two surface waves propagating at infinitely close frequencies $\omega - \delta\omega$ and $\omega + \delta\omega$ are combined, the resulting displacement field is the product of a very oscillatory term with propagation speed ω/k (the *phase velocity*), and a slowly oscillatory term with propagation speed $\delta\omega/\delta k$, coinciding (for sufficiently small $\delta\omega$) with $\frac{d\omega}{dk}$: the *group velocity*.

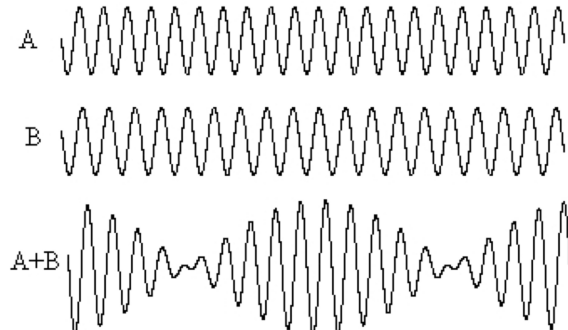


Figure 4.7: (A) and (B): two sinusoidal waves with slightly different frequencies. (A + B): their sum is a "beating pattern", or long-period envelope, which propagates at the group velocity $\frac{d\omega}{dk}$. A beating pattern is what you hear when you are tuning a guitar, and one string is a bit off with respect to the other.

The concept of group velocity: a more general derivation

We have seen that each component of a single-frequency Love or Rayleigh wave can be written $S(\omega) \cos[\omega(x/c - t)]$, with S a generic amplitude term. We are now interested in the combination of surface-wave signals at different frequencies. After selecting a discrete set of frequencies ω_i , this can be written

$$u(x, t) = \sum_{i=1}^{\infty} \int_{\omega_i - \epsilon}^{\omega_i + \epsilon} S(\omega) \cos \left[\omega \left(\frac{x}{c} - t \right) \right] \frac{1}{2\pi} d\omega, \quad (4.25)$$

with $\epsilon \ll \omega_i$. We next compact the notation by introducing $\varphi = \omega(\frac{x}{c} - t)$. Since ϵ is small, it makes sense to replace $\varphi(\omega)$ with its Taylor expansion around ω_i , i.e.

$$\varphi(\omega) \approx \varphi(\omega_i) + (\omega - \omega_i) \left[\frac{d\varphi}{d\omega} \right]_{\omega_i}, \quad (4.26)$$

where $[f(\omega)]_{\omega_i}$ denotes the value of f evaluated at $\omega = \omega_i$. After rewriting eq. (4.25) accordingly,

$$\begin{aligned} \int_{\omega_i-\epsilon}^{\omega_i+\epsilon} S(\omega) \cos \left[\omega \left(\frac{x}{c} - t \right) \right] d\omega &\approx \Re \left\{ \int_{\omega_i-\epsilon}^{\omega_i+\epsilon} S(\omega_i) e^{i\varphi(\omega_i)} e^{i(\omega-\omega_i)[\frac{d\varphi}{d\omega}]_{\omega_i}} d\omega \right\} \\ &= \Re \left\{ S(\omega_i) e^{i\varphi(\omega_i)} e^{-i\omega_i[\frac{d\varphi}{d\omega}]_{\omega_i}} \int_{\omega_i-\epsilon}^{\omega_i+\epsilon} e^{i\omega[\frac{d\varphi}{d\omega}]_{\omega_i}} d\omega \right\} \\ &= \Re \left\{ S(\omega_i) e^{i\varphi(\omega_i)} e^{-i\omega_i[\frac{d\varphi}{d\omega}]_{\omega_i}} \frac{1}{i[\frac{d\varphi}{d\omega}]_{\omega_i}} \left[e^{i\omega[\frac{d\varphi}{d\omega}]_{\omega_i}} \right]_{\omega_i-\epsilon}^{\omega_i+\epsilon} \right\} \\ &= \Re \left\{ S(\omega_i) e^{i\varphi(\omega_i)} \frac{1}{i[\frac{d\varphi}{d\omega}]_{\omega_i}} \left(e^{i\omega\epsilon[\frac{d\varphi}{d\omega}]_{\omega_i}} - e^{-i\omega\epsilon[\frac{d\varphi}{d\omega}]_{\omega_i}} \right) \right\} \\ &= S(\omega_i) \cos[\varphi(\omega_i)] \epsilon \frac{2 \sin(\epsilon [\frac{d\varphi}{d\omega}]_{\omega_i})}{\epsilon [\frac{d\varphi}{d\omega}]_{\omega_i}} \end{aligned}$$

where the operator \Re maps complex numbers to their real part, and the notation $[f(z)]_A^B = f(B) - f(A)$. The final expression that we obtained is compact enough that we can replace φ and its ω -derivative with their explicit form, i.e. $\varphi = \omega(x/c - t)$ and

$$\begin{aligned} \left[\frac{d\varphi}{d\omega} \right]_{\omega_i} &= \left[\frac{d}{d\omega} \left(\frac{\omega x}{c(\omega)} - \omega t \right) \right]_{\omega_i} \\ &= \left[\frac{x}{c(\omega)} - t - \frac{\omega x}{c^2(\omega)} \frac{dc}{d\omega} \right]_{\omega_i} \\ &= \frac{x}{c(\omega_i)} \left[1 - \frac{\omega_i}{c(\omega_i)} \frac{dc}{d\omega}(\omega_i) \right] - t \end{aligned}$$

If we then introduce a function

$$g(\omega) = \frac{c(\omega)}{1 - \frac{\omega}{c(\omega)} \frac{dc}{d\omega}}, \quad (4.27)$$

we can further write

$$\left[\frac{d\varphi}{d\omega} \right]_{\omega_i} = \frac{x}{g(\omega_i)} - t,$$

and after substituting into the above expression for eq. (4.25), we obtain

$$\int_{\omega_i-\epsilon}^{\omega_i+\epsilon} S(\omega) \cos \left(\omega \left[\frac{x}{c} - t \right] \right) d\omega \approx S(\omega_i) \cos \left(\omega_i \left[\frac{x}{c(\omega_i)} - t \right] \right) \epsilon \frac{2 \sin \left(\epsilon \left[\frac{x}{g(\omega_i)} - t \right] \right)}{\epsilon \left[\frac{x}{g(\omega_i)} - t \right]}. \quad (4.28)$$

The right-hand side of eq. (4.28) can be compared with eq. (4.24): it is the product of a wave of frequency ω and speed $c(\omega)$ and one of frequency $\epsilon \ll \omega$ and velocity $g(\omega_i)$. The latter factor, with much lower frequency, modulates the signal, similar to the factor $\cos(\delta\omega t - \delta kx_1)$ in eq. (4.24), and we call its speed g “*group velocity*”. Eq. (4.27) shows that, in the absence of dispersion (i.e. $dc/d\omega = 0$) phase and group velocities coincide. In practice, the values of c and g are always comparable, and the large difference in frequency results in a large difference in the wavelength of the phase and group terms.

In conclusion, the surface-wave signal can be written as a linear combination of terms associated with an arbitrary, discrete set of frequencies ω_i , propagating with speed $c(\omega_i)$ and modulated according to eq. (4.28), or formally:

$$u(x, t) = \sum_{i=1}^{\infty} S(\omega_i) \cos\left(\omega_i \left[\frac{x}{c(\omega_i)} - t \right]\right) \epsilon \frac{2 \sin\left(\epsilon \left[\frac{x}{g(\omega_i)} - t \right]\right)}{\epsilon \left[\frac{x}{g(\omega_i)} - t \right]}.$$

The modulation term also changes with frequency, and propagates with speed $g(\omega)$: the *group velocity*. In the Earth, the lower-frequency surface-wave signal, sensitive to deeper structure, is generally faster (see e.g. fig. 4.6), which makes the task of measuring group velocity and dispersion relatively easy.

4.5 Anisotropy

In a transversely isotropic (i.e. radially anisotropic) Earth, Love wavespeed depends primarily on *horizontally polarized* shear velocity: in fact, Love-wave displacement is parallel to the displacement associated with a horizontally polarized shear wave, propagating in the same direction (see again figure 4.2, top). Rayleigh wavespeed is, instead, a function of the values of compressional, and *vertically polarized* shear velocities: in fact, the direction of Rayleigh-wave displacement is always a combination of compressional (parallel to propagation) and vertically polarized shear displacement – no component in the horizontally polarized direction (figure 4.2, bottom).

Further Reading

- Aki, K., and P. G. Richards, *Quantitative Seismology, 2nd Edition*, University Science Books, 2002: section 7.1.
- Fowler, C. M. R., *The Solid Earth: An Introduction to Global Geophysics*, Cambridge University Press, New York, 2005.
- Lay, T. and T. C. Wallace, *Modern Global Seismology*, Academic Press, San Diego, 1995: chapter 4.
- Stein, S., and M. Wysession, *An Introduction to Seismology, Earthquakes, and Earth Structure*, Blackwell Science, Oxford, 2003.